JACC: CARDIOVASCULAR IMAGING VOL. 3, NO. 8, 2010

ISSN 1936-878X/$36.00
PUBLISHED BY ELSEVIER INC. DOI:10.1016/j.jcmg.2010.05.010

iLIGHTS

THE YEAR IN IMAGING

The Year in Intracoronary Imaging

James E. Muller, MD,* Neil J. Weissman, MD,† E. Murat Tuzcu, MD‡
Burlington, Massachusetts; Washington, DC; and Cleveland, Ohio

The past year was one of rapid development of novel intracoronary imaging methods with great potential to improve the care of patients. The impetus for the development of these new imaging methods has been a growing recognition of the limitations of coronary angiography—the dominant method for the assessment of coronary artery disease for the past 50 years. Examples of the remarkable images that can now be obtained in patients are shown in Figure 1 (1–3).

In most cases, the imaging techniques interrogate the coronary wall using either optical or acoustic signals delivered and retrieved by an intracoronary catheter. Although intravascular ultrasound (IVUS) and angioscopy have been used for decades, many of the methods under study are new, including optical approaches made possible by advanced lasers and optical detectors developed for use with the Internet (Table 1).

These new intracoronary imaging methods provide information often unobtainable by angiography that may improve treatment of both the *culprit lesion* and the nonculprit *vulnerable plaques* responsible for subsequent events (4).

Intracoronary Imaging to Improve Outcomes at the Culprit Lesion Site

Although the safety of coronary stenting has steadily improved the procedural complications of no or slow-reflow and peri-stenting infarction continue to occur in approximately 10% of patients. Within a year, restenosis is observed in 5% to 10% of patients, whereas stent thrombosis occurs in approximately 1% by 2 years. Intracoronary imaging may prove to be useful in reducing these complications by 1) improving the techniques of stent sizing and placement, 2) identifying the role of necrotic-core plaque as a cause of stent complications, and 3) assessing stent coverage and thrombosis.

Imaging to Improve Stent Sizing and Placement

Although angiographic guidance alone generally produces excellent outcomes, it has been proposed that the occasional complications (dissection, stent thrombosis, restenosis) result from a mismatch of vessel and stent size, failure to end the stent in an area of less plaque by IVUS, or failure to expand the stent leading to malapposition. Recently, Roy et al. (5) reported that IVUS guidance was an independent predictor of freedom from stent thrombosis, although there was no reduction in overall events. Doi et al. (6) demonstrated that reduced stent area determined by IVUS immediately after stenting is an independent predictor of subsequent in-stent restenosis. Gerber et al. (7) reported that IVUS-guided stent dilation led to larger lumen areas than did angiography-guided stenting. A randomized study of the value of IVUS guidance to optimize stenting has been initiated.

From *InfraReDx, Inc., Burlington, Massachusetts; †MedStar Health Research Institute at Washington Hospital Center and Georgetown University, Washington, DC; and the ‡Department of Cardiovascular Medicine, Cleveland Clinic Foundation, Cleveland, Ohio. Dr. Muller is CEO of InfraReDx, Inc. Dr. Weissman receives grant support from Boston Scientific.

Manuscript received January 20, 2010; revised manuscript received April 26, 2010, accepted May 13, 2010.

Necrotic Core Plaque as a Cause of Stenting Complications

Necrotic-core plaque and peri-stenting myocardial infarction (MI). Perhaps the greatest recent contribution of intracoronary imaging to understanding stenting complications has been the confirmation that balloon dilation of stenoses with necrotic cores produces emboli leading to peri-stenting MI. This phenomenon has been documented with the use of angioscopy (8), gray-scale IVUS (9), virtual histology (VH) IVUS (10), integrated backscatter (IB) IVUS (11), optical coherence tomography (OCT) (12) and near-infrared (NIR) spectroscopy (3).

Dilation of the necrotic core may also cause plaque shift that might in turn lead to side branch occlusion. Wei et al. (13) reported that balloon inflation led to a reduction in necrotic core (assessed by VH-IVUS), and a shift of plaque away from the ballooned area.

ABBREVIATIONS AND ACRONYMS

BMS = bare metal stent
ESS = endothelial shear stress
IB = integrated backscatter
IVUS = intravascular ultrasound
MACE = major adverse cardiac event
MI = myocardial infarction
NIR = near-infrared
OCT = optical coherence tomography
PCI = percutaneous coronary intervention
SES = sirolimus-eluting stent
TCFA = thin cap fibroatheroma
VH = virtual histology

Intracoronary Imaging and Late Stent Thrombosis

Failure of endothelial coverage of stent struts is a cause of thrombus and may occur more frequently when stents are placed over a necrotic core (14–16). OCT studies show that the incidence of malapposed struts is higher with sirolimus-eluting stents (SES) than with bare metal stents (BMS) (17,18). Tanigawa et al. (19) found that use of an SES was a predictor of malapposition, as were overlap stenting, post-dilation type C lesions, diabetes mellitus, and inflation pressure (Fig. 2).

Murakami et al. (20) found a greater incidence of in-stent thrombus in paclitaxel-coated stents compared with SES. An OCT follow-up study demonstrated that uncovered struts persist up to 2 years after SES implantation, suggesting the need for further follow-up (21). Hassan et al. (22) found that the risk of acquired stent malapposition detected by IVUS was 4-fold higher with DES than BMS and the risk of very late stent thrombosis was higher in those with late malapposition. Takano et al. (23) observed a very high incidence of mural thrombus as detected by angioscopy 6 months after DES implantation despite angioscopic evidence of stent coverage by neointima. The discordance between frequent mural thrombus and infrequent clinical stent thrombosis is presumably due to antiplatelet therapy (Fig. 3).

Finn et al. (14) suggested that BMS, because they endothelialize more readily than DES, may be preferred for a necrotic-core plaque when other factors favoring a BMS or a DES are equally balanced. These conclusions were based on autopsy findings not preceded by in vivo imaging. There is extensive clinical trial evidence supporting the safety of DES in acute coronary syndrome cases in which necrotic cores are likely to have been stented (24).

Abbott (25) noted that although both OCT and angioscopy can provide information about the presence of tissue over a stent, the tissue observed is not always thrombo-resistant endothelium. Higo et al. (26) found by angioscopy that neointima within an SES became increasingly yellow by 10 months and was associated with mural thrombus, whereas neointima within a BMS was more likely to be white and not associated with thrombus. Murakami et al. (27) also reported that neointima within an SES was yellow on angioscopy and showed OCT signs of a lipid-core plaque that were not observed in neointima over a BMS. Nakazawa et al. (28) noted that the angioscopic findings of yellow after SES placement and pathologic observations suggest that certain stents might create a "nouveau atherosclerosis" with unfavorable long-term consequences.

Intracoronary imaging, although not currently capable of detecting endothelial cells or measuring their function, is likely to play an important role in resolving the problem of late stent thrombosis because of its ability to identify thrombus and stent coverage. The intracoronary imaging findings that struts are often uncovered, that mural thrombus is frequent, and that even visible neointima may not be functional have implications for the duration of antiplatelet therapy and indicate the need for improved stent technology. It seems that the stent thrombosis rate may be lower with newer stents designed with less metal (leading to improved endothelialization) (29). Bioabsorable stents remove the problem of the prolonged presence of a thrombogenic substance requiring development of new thrombo-resistant endothelium (30,31). The new methods of intracoronary imaging may be useful in the evaluation of new types of stents designed to improve endothelial coverage and decrease stent thrombosis.

Identification of Vulnerable Plaque at Nonculprit Sites

Although detection of vulnerable plaque—the presumed cause of a subsequent coronary event from a

nonculprit lesion—is a major goal of intracoronary imaging, the term has been used with 4 different meanings (Table 2). The original definition described a concept (a plaque prone to disruption and thrombosis) (32), whereas angiographic studies indicated that such plaques are not necessarily stenotic at baseline (33,34). Autopsy data indicated that an inflamed thin cap fibroatheroma (TCFA) is likely to be a vulnerable plaque. The recent PROSPECT (Predictors of Response to Cardiac Resynchronization Therapy) study (37) used a broader definition that includes plaques likely to cause progressive angina. It could include a plaque not stented at the initial percutaneous coronary intervention (PCI) that caused angina with or without a minor nonthrombotic increase in stenosis during follow-up.

In September 2009, the results of the PROSPECT study, the first prospective, large-scale, long-term attempt to identify vulnerable plaques, were reported at the Transcatheter Cardiovascular Therapeutics (TCT) annual meeting (37). The study was conducted in 700 patients receiving PCI for an acute coronary syndrome. The PROSPECT study used the new, broad definition of a vulnerable plaque as a plaque, not the original culprit at the index event, likely to cause a major adverse cardiac event (MACE) after PCI. MACE was defined as cardiac death, cardiac arrest, MI, unstable angina, or increasing angina requiring revascularization or rehospitalization.

The primary findings were as follows: 1) by 3.4 years, 20.4% of the patients experienced a second event, only 4.9% of which were "hard" (cardiac death, cardiac arrest, and MI), leaving 15.5% with progressive angina or unstable angina (Fig. 4). 2) Approximately half of the events occurred at the previous culprit lesion site and half at sites not treated at the initial PCI. 3) Sites with a plaque burden of >70% as shown by IVUS, a VH-TCFA, and lumen area <4 mm^2 had a 17% risk of causing an event versus a risk of <2% for plaques without those 3 features (37).

These results are provocative. Although the rates of cardiac death and MI were lower than expected (presumably due to medical therapy including antithrombotic agents), the PROSPECT study demonstrated the ability of imaging to identify nonstented sites likely to cause MACEs after stenting of a culprit lesion. The PROSPECT study did not identify novel features of plaques prone to disruption and thrombosis—the original definition of vulnerable plaque—for 2 reasons. First, the broad definition of vulnerable plaque used—a plaque likely to cause an MACE event after stenting—included increasing angina that may not have been due to plaque disruption and thrombosis. Second, the successful predictors that included the finding of a lumen area <4 mm^2 provide relatively little new information because such narrowing is generally considered a sign of a flow-limiting stenosis in need of treatment regardless of future vulnerability.

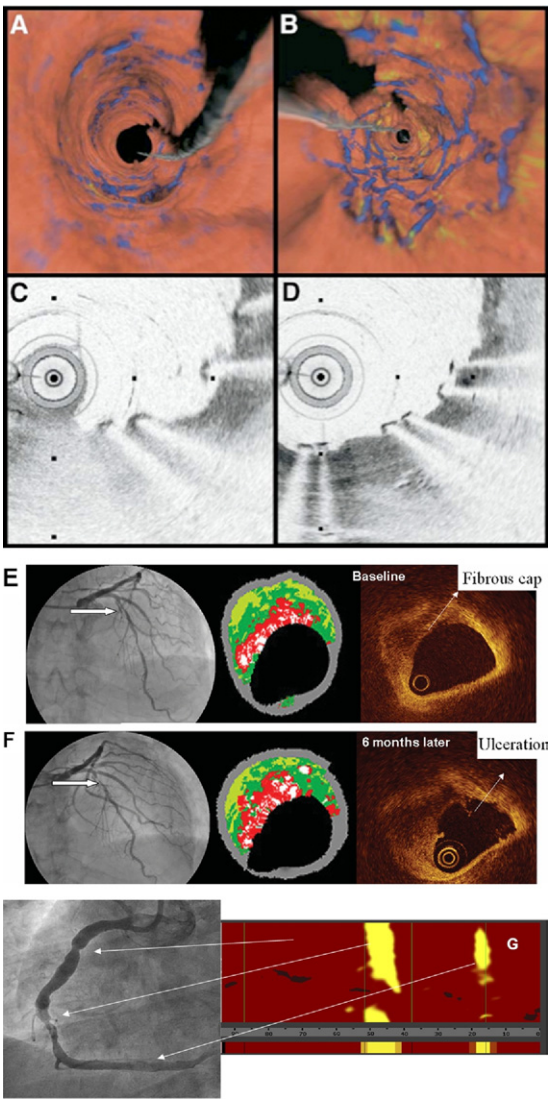

Figure 1. Novel Intracoronary Imaging Devices

(A) A fly-through view obtained by optical Fourier domain imaging showing a stent implanted 9 years earlier and a new stent **(B)** (1). **(C and D)** Cross-sectional view showing struts of the 2 stents. **(E)** Angiogram showing a 50% stenosis at a site of a thin-cap fibroatheroma (TCFA) by both virtual histology **(center)** and optical coherence tomography (OCT) **(right)** (2). **(F)** Six months later, rupture of the TCFA, documented by OCT, led to unstable angina. **(G)** Near-infrared spectroscopic data showing a circumferential lipid-core plaque at a stenosis; balloon dilation led to severe no-reflow, presumably due to embolization of plaque contents (3).

Table 1. Intracoronary Imaging Techniques

Used in Patients for >2 Decades	Developed and Used in Patients Within the Past Decade	In Development
Angioscopy	VH-IVUS	Raman spectroscopy
Gray-scale IVUS	IB-IVUS	Time resolved laser-induced fluorescence spectroscopy
	OCT	Fluorescence angioscopy
	OFDI-OCT	Molecular imaging
	Near-infrared spectroscopy	

IB = integrated backscatter; IVUS = intravascular ultrasound; OCT = optical coherence tomography; OFDI = optical Fourier domain imaging; VH = virtual histology.

Full interpretation of the PROSPECT study will not be possible until multiple publications are available describing the results of this extensive trial. For the present, the PROSPECT study investigators stated that the positive results of the trial did not support the routine performance of 3-vessel IVUS to identify vulnerable plaques.

Shear Stress to Identify Sites Vulnerable to Becoming Vulnerable

The plaques suspected to be vulnerable are not randomly distributed throughout the coronary tree. As would be expected from extensive vascular biology research showing the atherogenic effects of low endothelial shear stress (ESS), Chatzizisis et al. (38) found in swine that low ESS detected in vivo after 23 weeks of an atherogenic diet predicted the development by 30 weeks of lipid-laden high-risk plaques. Sites with low ESS also showed enhanced activity of matrix-degrading proteases—enzymes implicated in formation of plaques with necrotic cores (39). Conversely, Gijsen et al. (40) found that maximum plaque deformability was found at sites exposed to the *highest* ESS (40). The varied findings demonstrate the complex interactions among ESS, the stage of development of the plaque, expansive remodeling, and the development of stenosis.

Identification of TCFAs

Abundant pathologic and clinical data (36) indicate that TCFAs, which have many features attractive for imaging (Table 3), are likely to be vulnerable plaques. Different intracoronary imaging methods have different strengths and weaknesses for detecting the various features of interest. We focus mainly on those technologies capable of detection of the necrotic core, the largest feature of TCFA and perhaps the most attractive target for imaging.

Detection of the Necrotic Core

IVUS-based methods. IVUS, which is in widespread use to identify plaque structure and stent features, can also be used for plaque characterization. The 4 IVUS-based methods that have been used to identify necrotic core—gray-scale IVUS, VH-IVUS, IB-IVUS, and palpography—were reviewed recently (41).

Lee et al. (42) reported that attenuated plaque, defined as hypoechoic plaque not due to calcium shadowing and considered to represent necrotic core by gray-scale IVUS, was never found in stable patients, but was observed in 39.9% of patients with ST-segment elevation MI, supporting the association of attenuated plaque with necrotic-core plaque and/or a platelet thrombus. In contrast, Bayturan et al. (43) found that attenuated plaques were found with equal frequency in stable and unstable patients and not associated with subsequent coronary events.

As noted previously, patients with attenuated plaque were also more likely to experience a cardiac enzyme elevation after PCI, suggesting the presence of a necrotic core at the dilated site.

The limitations of gray-scale IVUS for tissue characterization led to the development of VH-IVUS and IB-IVUS, which use information in the radiofrequency backscattered IVUS signal not displayed on the gray-scale screen.

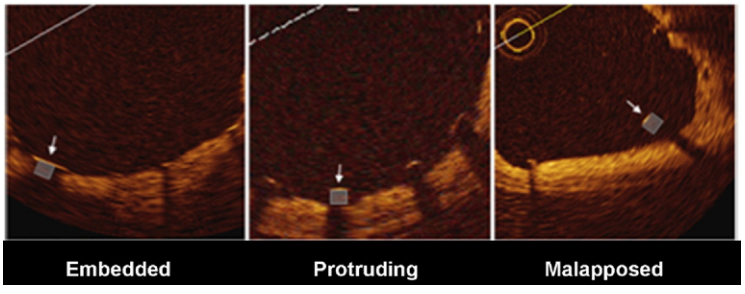

Figure 2. Strut Apposition as Determined by OCT

Arrows indicate stent struts. Reprinted, with permission, from Tanigawa et al. (19). Abbreviation as in Figure 1.

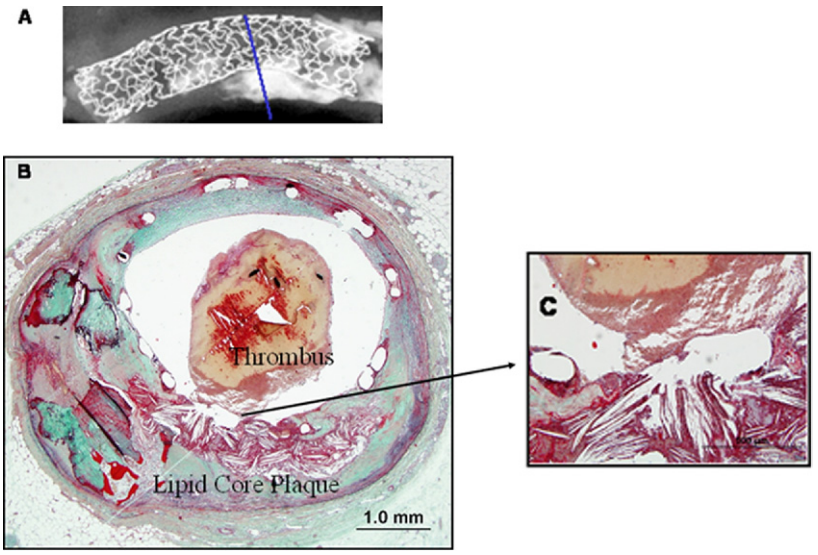

Figure 3. Fatal Thrombus Within a Drug-Eluting Stent Located Over a Lipid-Core Plaque

(A) Postmortem X-ray of overlapping stents. **(B)** Cross section showing stent struts, a lipid-core plaque with cholesterol crystals, and an intracoronary thrombus. **(C)** Close up of area shown in **(B)**. Struts at 12 o'clock, which appose normal tissue, are well covered by neointima, whereas struts at 6 o'clock, which appose the lipid core, are exposed (14).

A VH-TCFA has been defined as a plaque that in 3 adjacent cross sections has a plaque burden >40% and a confluent necrotic core occupying ≥10% of the cross section of the artery that is in contact with the lumen (37). In studies of groups of patients, this definition has led to identification of plaques showing the expected features of necrotic cores. VH-TCFAs have been found to be more frequent in lesions causing acute coronary syndromes (44) and lesions causing embolization-related peri-stenting infarction (10). Similar studies are available for IB-IVUS. Okubo et al. (45) reported that IB-IVUS performed better than VH-IVUS in a correlation with a histologic gold standard.

The presence of a VH-TCFA is currently being used to select the plaques randomly assigned to standard care or treatment with a self-expanding stent designed for non–flow-limiting plaques suspected to be vulnerable (46).

Future improvements in IVUS technology include the possibility that higher frequency imaging will lead to improved spatial resolution and improved detection of lumen and external elastic membrane borders.

Optical methods. **INTRACORONARY ANGIOSCOPY.** In 1995, Uchida et al. (47) reported the first study linking plaque composition to patient outcome. Patients with glistening yellow plaques, presumably lipid-core plaques, had an increased incidence of future events. Later Ohtani et al. (48) linked the number of yellow plaques to the risk of future events, thereby detecting vulnerable patients. In 2009, Uchida (49) introduced fluorescence angioscopy for molecular imaging. Using

Table 2. Four Definitions of Vulnerable Plaque

Source (Ref. #)	Definition	Feature
Studies of triggering of onset of coronary events (32)	A plaque prone to disruption and thrombosis after a triggering event.	A functional definition independent of histologic type
Angiographic studies (33,34)	As above, but the plaque need not be stenotic at baseline	This type of vulnerable plaque could not be detected by ischemia testing
Autopsy studies after coronary events (35,36)	An inflamed TCFA	A suspected vulnerable plaque and a good target for imaging
The PROSPECT study, a post-ACS and PCI natural history study (37)	A plaque likely to cause a new coronary event including cardiac death, MI, unstable angina, and progressive angina	A broader definition of vulnerable plaque that does not require disruption and thrombosis because increased angina is an end point

ACS = acute coronary syndrome; MI = myocardial infarction; PCI = percutaneous coronary intervention; TCFA = thin cap fibroatheroma.

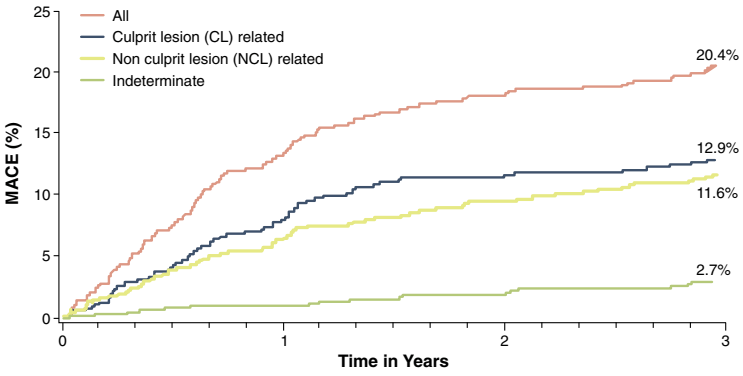

Figure 4. MACE During Follow-up in the PROSPECT Study

During 3 years post-stenting for acute coronary syndrome, 20.4% of patients experienced a major adverse cardiac event (MACE). Approximately half of the subsequent events came from the stented site, with the other half coming from sites not treated at the initial percutaneous coronary intervention. Adapted from TCT Daily Staff (37).

colorimetric angioscopic yellow as a gold standard, Yamamoto et al. (50) found that the sensitivity, specificity, and accuracy of VH-IVUS for TCFA were 68%, 81%, and 75%, respectively.

OCT and fourier domain OCT. OCT provides high-resolution (10 μm) images of arteries (51). Second-generation Fourier-domain OCT permits performance of OCT, which requires removal of blood from the field of view, with only a single flush (52). Using Fourier-domain OCT, Tearney et al. (1) were able to obtain microscopic images of the coronary wall including identification of macrophages in a cap covering a lipid pool. Kataiwa et al. (53) found that the new nonocclusive method is safe and provides image quality equal to that obtained with the balloon occlusion method.

Fujii et al. (54) found that OCT TCFAs were more frequent at the culprit site than at remote sites in MI patients and that MI patients were more likely than stable patients to have multiple TCFAs.

Xu et al. (55) demonstrated that a combination of backscattering and attenuation coefficient measurements could be used to improve tissue characterization by OCT. Additional future improvements include improved depth of penetration, which is currently limited to approximately 2 mm.

Multimodality imaging. OCT AND VH-IVUS. Sawada et al. (2) interrogated plaques with both VH-IVUS and OCT to identify compositional and structural features. Of the 126 plaques examined, 61 showed TCFAs by VH-IVUS and 36 were classified as

Table 3. Histologic Features of Suspected Vulnerable Plaques

Type	Features
Inflamed thin-cap fibroatheroma, most frequent type and present in 60% to 70% of ACS cases	Necrotic core (lipid core)
	Thin cap <65 μm
	Inflammation
	Increased vasa vasorum
	Expansive remodeling
	Increased plaque burden
	Intraplaque hemorrhage
	Spotty calcification
	Luminal narrowing
Erosion site, present in 20% to 30% of events, more frequent in women and younger patients with ACS	Increased proteoglycans
Calcified nodule, present in <3% of patients with ACS	Extensive calcification protruding into lumen
Plaque with a mural thrombus not producing a significant stenosis	Considered to be a site of subsequent thrombosis because many plaques causing events show repeated episodes of disruption and thrombosis

Abbreviation as in Table 2.

TCFAs by OCT. In the combined analysis, 28 were diagnosed as TCFAs by both methods. During follow-up, 3 of these sites, which did not have a flow-limiting stenosis at the initial study, demonstrated stenosis progression requiring PCI (Fig. 1). The authors conclude that the combined use of OCT and VH-IVUS, preferably in a single catheter, might be a feasible approach for detecting TCFA.

Gonzalo et al. (56) also used both OCT and VH-IVUS to determine the frequency and distribution of high-risk plaques at bifurcations. This dual examination demonstrated that the proximal rim of the side branch ostium was the more likely region to contain a thin fibrous cap and a larger necrotic core.

IVUS, OCT, AND ANGIOSCOPY. Kubo et al. (57) used 3 methods—angioscopy, IVUS, and OCT—in patients with AMI. Intracoronary thrombus at the culprit site was observed in all cases by OCT and angioscopy, whereas IVUS identified thrombus in only 33% of cases. The incidence of plaque rupture was by 73% with OCT, 47% with angioscopy, and 40% with IVUS.

Diffuse reflectance NIR spectroscopy. A catheter-based NIR spectroscopy system has been developed to identify lipid-core plaque in coronary arteries (58). An NIR scan is performed through blood in a manner similar to that used for IVUS and is displayed as a map of the artery called a chemogram (59). The system, which was validated by comparison of NIR chemograms with histologic results in human coronary autopsy specimens and with a clinical study (59,60), has now been used in >700 patients. Although the chemogram provides accurate information about the presence of lipid-core plaque, it does not provide a structural image.

Raman spectroscopy. Raman spectroscopy is similar to diffuse reflectance NIR spectroscopy, but it relies on a more specific yet weaker signal created by photons that undergo a Raman shift within the tissue interrogated. A catheter-based system has obtained useful Raman signals from inside a human coronary autopsy specimen implanted in a living swine, but there are at present no reports of the use of the system in patients (61).

Magnetic resonance imaging. A catheter that contained both the device to generate the magnetic field and the coil to send and receive radiofrequency signals was able to identify lipid-core plaque in patients (62). However, the large size of the catheter and long processing time limited its clinical utility, and the system is no longer manufactured for this use.

Intravascular thermography. There have been attempts to identify necrotic-core plaque by measuring intracoronary temperature elevations. It was found, however, that the small thermal gradients associated with inflamed plaques are difficult to measure in flowing blood. A review of thermography was recently published (63).

MEASUREMENT OF CAP THICKNESS. The observation of thin caps in plaques that have ruptured has led to attempts to measure cap thickness in vivo. Cap thickness has been estimated by VH-IVUS, but the 100-μm limit of resolution of IVUS does

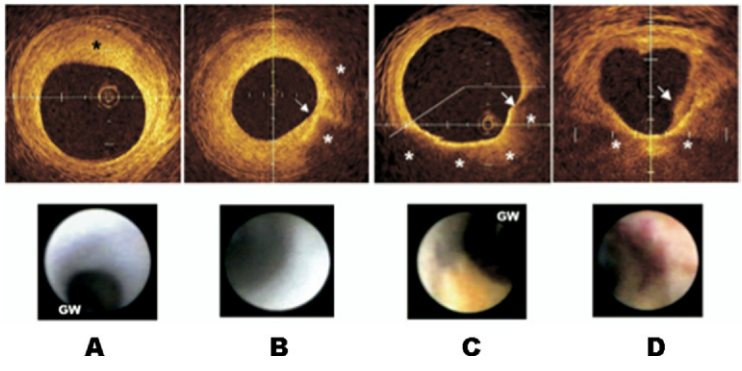

Figure 5. OCT and Angioscopic Images in a Patient

Optical coherence tomography (OCT) images **(upper panel)** and angioscopic images **(lower panel)**. **(A and upper panel)** A white plaque by angioscopy is diagnosed as a fibrous plaque (*) by OCT. **(B and upper panel)** A white plaque by angioscopy contains a lipid core (*) under a relatively thick (130 μm) fibrous cap. **(C and upper panel)** A dark yellow plaque by angioscopy is shown by OCT to contain a lipid core (*) with a thin (20 μm) fibrous cap **(arrow)**. The arc of lipid is indicated by the angle between the 2 white lines. **(D and upper panel)** Angioscopy shows a red thrombus over a yellow plaque. OCT shows a protruding thrombus **(arrow)** overlying a lipid core with a thin cap (*). Reprinted, with permission, from Takano et al. (64). GW = guidewire; other abbreviation as in Figure 1.

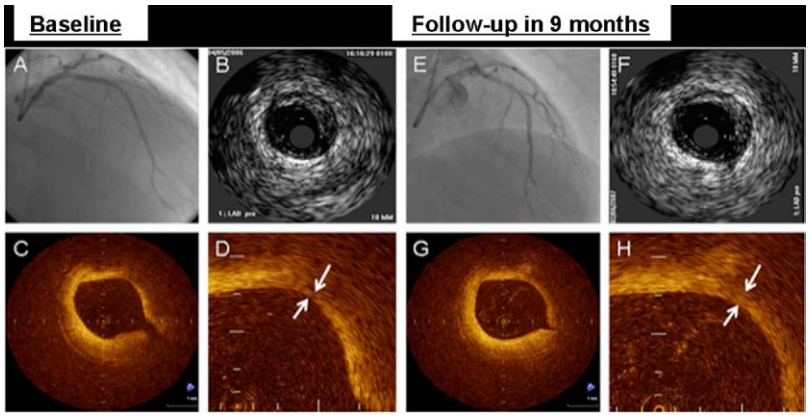

Figure 6. Effect of Statin Therapy on Cap Thickness

Angiographic **(A and E)**, intravascular ultrasound **(B and F)**, and OCT **(C–H)** images at baseline and after 9 months of statin therapy (66). OCT shows an increase in cap thickness **(D, H, arrows)** from 110 μm at baseline **(D)** to 320 μm at 9-month follow-up **(H)**.

not permit exact measurement of the thin cap of interest. OCT and angioscopy, however, have greater resolution and have been used for more direct measurements of cap thickness. Takano et al. (64) found the expected inverse relationship between the intensity of yellow coloring (assessed by angioscopy) of the plaque and cap thickness as measured by OCT (Fig. 5). Plaques with the highest yellow color grade were found to have a cap thickness of only 40 ± 14 μm.

Identification of Other Plaque Morphologies Associated With Coronary Events

Although the effort to identify TCFAs has received the greatest attention in the quest for identification of vulnerable plaques, pathologic studies indicate that as many as 30% of clinical events occur at erosion sites and a much smaller number occur at the site of calcified nodules (Table 3).

In vivo identification of erosion sites lags behind the recent success in identifying necrotic cores. Fatal thrombi over erosion sites are more likely to be recurrent than thrombi over ruptured TCFAs (65). Although OCT may be able to identify some erosion sites, imaging of sites prone to erosion will require more detailed assessment of local molecular processes than is possible with current intracoronary imaging techniques (Fig. 6) (66).

Molecular Imaging of Coronary Atherosclerotic Plaques

A full understanding of the status of coronary atherosclerosis in a patient will require information about the molecular and cellular processes within plaques (67,68). Fortunately, progress in molecular and cellular imaging indicates that invasive and even noninvasive techniques offer promise for identification of molecular processes in the coronary plaques of patients (69–71).

Table 4. Comparison of Intracoronary Imaging Modalities

	IVUS (40 MHz)	VH (20 MHz)	OCT	Near-infrared Spectroscopy	Angioscopy
Axial resolution, μm	100	200	10	NA	10–50
PCI (stent expansion and complications)	++	±	++	−	±
Necrotic core	±	+	+	++	+
Detection of thin cap	±	+	++	−	+
Thrombus	±	−	+	−	++
Stent tissue coverage	+	+	++	−	++
Expansive remodeling	++	++	−	−	−
Measurement through blood	++	++	−	+	−

Adapted from Maehara et al. (41)
++ = excellent; + = good; ± = possible; − = impossible; IVUS = intravascular ultrasound; NA = not available; VH = virtual histology; other abbreviations as in Tables 1 and 2.

Chang and Jaffer (71) injected an NIR fluorescence agent that is activated by proteases into atherosclerotic rabbits. Catheter interrogation of the iliac arteries then demonstrated activation of the agent, indicating the presence of protease activity in plaques. The agent colocalized with immunoreactive macrophages and cathepsin B, thereby identifying inflammation.

Conclusions

Intracoronary imaging is an active research field with great potential to improve patient care. In the effort to detect vulnerable plaque, the most significant development is the continued accumulation of evidence that certain plaques are more likely to cause clinical events and therefore deserve the term vulnerable; the evidence includes the early angioscopic study by Uchida (47), the recent observation that 3 patients with TCFAs by both VH-IVUS and OCT measures experienced events (2), and the finding in the PROSPECT study that certain sites were prone to cause clinical events (37).

As is apparent from Table 4, the various intracoronary imaging methods are complementary. Hence, extensive efforts are under way to build combined imaging devices. The improved characterization of coronary plaques with these new techniques has the potential to improve the selection of therapy for patients, reduce the complications of stenting, and identify vulnerable plaques so they may be treated before they cause an event. Multiple clinical studies are in progress to determine how these new diagnostic capabilities might be used to improve the daily care of patients with coronary artery disease.

Acknowledgments

We are grateful for the assistance of Ruth Potwin in preparation of the manuscript.

Reprint requests and correspondence: Dr. E. Murat Tuzcu, Department of Cardiology, Cleveland Clinic Foundation, Desk F-25, 9500 Euclid Avenue, Cleveland, Ohio 44195-0001. *E-mail: tuzcue@ccf.org.*

REFERENCES

1. Tearney GJ, Waxman S, Shishkov M, et al. Three-dimensional coronary artery microscopy by intracoronary optical frequency domain imaging. J Am Coll Cardiol Img 2008;1:752–61.
2. Sawada T, Shite J, Garcia-Garcia HM, et al. Feasibility of combined use of intravascular ultrasound radiofrequency data analysis and optical coherence tomography for detecting thin-cap fibroatheroma. Eur Heart J 2008;29:1136–46.
3. Goldstein JA, Grines C, Fischell T, et al. Coronary embolization following balloon dilation of lipid-core plaques. J Am Coll Cardiol Img 2009;2:1420–4.
4. Kern MJ, Narula J. Looking into the vessel: the more you see, the more you want to see. J Am Coll Cardiol Img 2008;1:556–9.
5. Roy P, Steinberg DH, Sushinsky SJ, et al. The potential clinical utility of intravascular ultrasound guidance in patients undergoing percutaneous coronary intervention with drug-eluting stents. Eur Heart J 2008;29:1851–7.
6. Doi H, Maehara A, Mintz GS, et al. Impact of post-intervention minimal stent area on 9-month follow-up patency of paclitaxel-eluting stents: an integrated intravascular ultrasound analysis from the TAXUS IV, V, and VI and TAXUS ATLAS Workhorse, Long Lesion, and Direct Stent Trials. J Am Coll Cardiol Intv 2009;2:1269–75.
7. Gerber RT, Latib A, Ielasi A, et al. Defining a new standard for IVUS optimized drug eluting stent implantation: the PRAVIO study. Catheter Cardiovasc Interv 2009;74:348–56.
8. Mizote I, Ueda Y, Kodama K, et al. Distal protection improved reperfusion and reduced left ventricular dysfunction in patients with acute myocardial infarction who had angioscopically defined ruptured plaque. Circulation 2005;112:1001–7.
9. Okura H, Taguchi H, Kubo T, et al. Atherosclerotic plaque with ultrasonic attenuation affects coronary reflow and infarct size in patients with acute coronary syndrome: an intravascular ultrasound study. Circ J 2007;71:648–53.
10. Hong YJ, Jeong MH, Choi YH, et al. Impact of plaque components on no-reflow phenomenon after stent deployment in patients with acute coronary syndrome: a virtual histology-intravascular ultrasound analysis. Eur Heart J 2009 Feb 19 [E-pub ahead of print].
11. Uetani T, Amano T, Ando H, et al. The correlation between lipid volume in the target lesion, measured by integrated backscatter intravascular ultrasound, and post-procedural myocardial infarction in patients with elective stent implantation. Eur Heart J 2008;29:1714–20.
12. Tanaka A, Imanishi T, Kitabata H, et al. Lipid-rich plaque and myocardial perfusion after successful stenting in patients with non-ST segment elevation acute coronary syndrome: an optical coherence tomography study. Eur Heart J 2009;30:1348–55.
13. Wei H, Schiele F, Descotes-Genon, V, et al. Changes in unstable coronary atherosclerotic plaque composition after balloon angioplasty as determined by analysis of intravascular ultrasound radiofrequency. Am J Cardiol 2008;101:173–8.
14. Finn AV, Nakazawa G, Ladich E, et al. Does underlying plaque morphology play a role in vessel healing after drug-eluting stent implantation? J Am Coll Cardiol Img 2008;1:485–8.
15. Higo T, Ueda Y, Oyabu J, et al. Atherosclerotic and thrombogenic neointima formed over sirolimus drug-eluting stent: an angioscopic study. J Am Coll Cardiol Img 2009;2:616–24.
16. Jiménez-Valero S, Moreno R, Sánchez-Recalde A. Very late drug-eluting stent thrombosis related to incomplete stent endothelialization: in-vivo demonstration by optical coherence tomography. J Invasive Cardiol 2009;21:488–90.

17. Xie Y, Takano M, Murakami D, et al. Comparison of neointimal coverage by optical coherence tomography of a sirolimus-eluting stent versus a bare-metal stent three months after implantation. Am J Cardiol 2008;102: 27–31.
18. Chen BX, Ma FY, Luo W, et al. Neointimal coverage of bare-metal and sirolimus-eluting stents evaluated with optical coherence tomography. Heart 2008;94:566–70.
19. Tanigawa J, Barlis P, Dimopoulos K, Dalby M, Moore P, Di Mario C. The influence of strut thickness and cell design on immediate apposition of drug-eluting stents assessed by optical coherence tomography. Int J Cardiol 2009;134:180–8.
20. Murakami D, Takano M, Yamamoto M, et al. Advanced neointimal growth is not associated with a low risk of in-stent thrombus. Optical coherence tomographic findings after first-generation drug-eluting stent implantation. Circ J 2009;73:1627–34.
21. Takano M, Yamamoto M, Inami S, et al. Long-term follow-up evaluation after sirolimus-eluting stent implantation by optical coherence tomography: do uncovered struts persist? J Am Coll Cardiol 2008;51:968–9.
22. Hassan AK, Bergheanu SC, Stijnen T, et al. Late stent malapposition risk is higher after drug-eluting stent compared with bare-metal stent implantation and associates with late stent thrombosis. Eur Heart J 2010;31; 1172–80.
23. Takano M, Yamamoto M, Murakami D, et al. Lack of association between large angiographic late loss and low risk of in-stent thrombus. Circ Cardiovasc Interv 2008;1:20–7.
24. Stone GW, Lansky AJ, Pocock SJ, et al. Paclitaxel-eluting stents versus bare-metal stents in acute myocardial infarction. N Engl J Med 2009;360: 1946–59.
25. Abbott JD. Revealing the silver and red lining in drug-eluting stents with angioscopy. Circ Cardiovasc Interv 2008;1:7–9.
26. Higo T, Ueda Y, Oyabu J, et al. Atherosclerotic and thrombogenic neointima formed over sirolimus drug-eluting stent: an angioscopic study. J Am Coll Cardiol Img 2009; 2:616–24.
27. Murakami D, Takano M, Yamamoto M, et al. Novel neointimal formation over sirolimus-eluting stents identified by coronary angioscopy and optical coherence tomography. J Cardiol 2009;53:311–3.
28. Nakazawa G, Vorpahl M, Finn AV, Narula J, Virmani R. One step forward and two steps back with drug-eluting-stents: from preventing restenosis to causing late thrombosis and nouveau atherosclerosis. J Am Coll Cardiol Img 2009;2:625–8.
29. Stone GW, Midei M, Newman W, et al. SPIRIT III Investigators. Randomized comparison of everolimus-eluting and paclitaxel-eluting stents. Circulation 2009;119:680–6.
30. Serruys PW, Ormiston JA, Onuma Y, et al. A bioabsorbable everolimus-eluting coronary stent system (ABSORB): 2-year outcomes and results from multiple imaging methods. Lancet 2009;373:897–910.
31. Waksman R, Erbel R, Di Mario C, et al. PROGRESS-AMS. Early- and long-term intravascular ultrasound and angiographic findings after bioabsorbable magnesium stent implantation in human coronary arteries. J Am Coll Cardiol Intv 2009;2:312–20.
32. Muller J, Tofler G, Stone P. Circadian variation and triggers of onset of acute cardiovascular disease. Circulation 1989;79:733–43.
33. Ambrose JA, Tannenbaum MA, Alexopoulos D, et al. Angiographic progression of coronary artery disease and the development of myocardial infarction. J Am Coll Cardiol 1988; 12:56–62.
34. Little WC, Constantinescu M, Applegate RJ, et al. Can coronary angiography predict the site of a subsequent myocardial infarction in patients with mild-to-moderate coronary artery disease? Circulation 1988; 78:1157–66.
35. Falk E. Plaque rupture with severe pre-existing stenosis precipitating coronary thrombosis. Characteristics of coronary atherosclerotic plaques underlying fatal occlusive thrombi. Br Heart J 1983;50:127–34.
36. Virmani R, Kolodgie FD, Burke AP, Farb A, Schwartz SM. Lessons from sudden coronary death: a comprehensive morphological classification scheme for atherosclerotic lesions. Arterioscler Thromb Vasc Biol 2000;20: 1262–75.
37. TCT Daily Staff. PROSPECT assesses impact of non-culprit lesions. September 25, 2009. Available at: http://www.tctmd.com/show.aspx?id=86174. Accessed November 20, 2009.
38. Chatzizisis YS, Jonas M, Coskun AU, et al. Prediction of the localization of high-risk coronary atherosclerotic plaques on the basis of low endothelial shear stress. Circulation 2008;117: 993–1002.
39. Koskinas KC, Chatzizisis YS, Baker AB, Edelman ER, Stone PH, Feldman CL. The role of low endothelial shear stress in the conversion of atherosclerotic lesions from stable to unstable plaque. Curr Opin Cardiol 2009;24:580–90.
40. Gijsen FJH, Wentzel JJ, Thury A, et al. Strain distribution over plaques in human coronary arteries relates to shear stress. Am J Physiol Heart Circ Physiol 2008;295:H1608–14.
41. Maehara A, Mintz GS, Weissman NJ. Advances in intravascular imaging. Circ Cardiovasc Interv 2009;2: 482–90.
42. Lee SY, Mintz GS, Kim SY, et al. Attenuated plaque detected by intravascular ultrasound. J Am Coll Cardiol Intv 2009;2:65–72.
43. Bayturan O, Tuzcu EM, Nicholls SJ, et al. Attenuated plaque at nonculprit lesions in patients enrolled in intravascular ultrasound atherosclerosis progression trials. J Am Coll Cardiol Intv 2009;2:672–8.
44. Missel E, Mintz GS, Carlier SG, et al. Necrotic-core and its ratio to dense calcium are predictors of high-risk non-ST-elevation acute coronary syndrome. Am J Cardiol 2008;101: 573–8.
45. Okubo M, Kawasaki M, Ishihara Y, et al. Tissue characterization of coronary plaques: comparison of integrated backscatter intravascular ultrasound with virtual histology intravascular ultrasound. Circ J 2008;72:1631–9.
46. Ramcharitar S, Gonzalo N, van Geuns RJ, et al. First case of stenting of a vulnerable plaque in the SECRITT I trial-the dawn of a new era? Nat Rev Cardiol 2009;6:374–8.
47. Uchida Y. Prediction of acute coronary syndromes by percutaneous angioscopy in patients with stable angina. Am Heart J 1995;130:195–203.
48. Ohtani T, Ueda Y, Mizote I, et al. Number of yellow plaques detected in a coronary artery is associated with future risk of acute coronary syndrome: detection of vulnerable patients by angioscopy. J Am Coll Cardiol 2006;47:2194–200.
49. Uchida Y. Coronary angioscopy: from tissue imaging to molecular imaging. Curr Cardiovasc Imaging Rep 2009;2: 284–92.
50. Yamamoto M, Takano M, Okamatsu K, et al. Relationship between thin cap fibroatheroma identified by virtual histology and angioscopic yellow plaque in quantitative analysis with colorimetry. Circ J 2009;73:497–502.
51. Jang I, Tearney GJ, MacNeill B, et al. In vivo characterization of coronary atherosclerotic plaque by use of optical coherence tomography. Circulation 2005;111:1551–5.
52. Barlis P, Schmitt JM. Current and future developments in intracoronary optical coherence tomography imaging. EuroIntervention 2009;4:529–33.

53. Kataiwa H, Tanaka A, Kitabata H, et al. Head-to-head comparison between the conventional balloon occlusion method and the non-occlusion method for optical coherence tomography. Int J Cardiol 2009 Aug 5 [E-pub ahead of print].
54. Fujii K, Masutani M, Okumura T, et al. Frequency and predictor of coronary thin-cap fibroatheroma in patients with acute myocardial infarction and stable angina pectoris: a 3-vessel optical coherence tomography study. J Am Coll Cardiol 2008;52:787–8.
55. Xu C, Schmitt JM, Carlier SG, Virmani R. Characterization of atherosclerosis plaques by measuring both backscattering and attenuation coefficients in optical coherence tomography. J Biomed Opt 2008;13:034003.
56. Gonzalo N, Garcia-Garcia HM, Regar E, et al. In vivo assessment of high-risk coronary plaques at bifurcations with combined intravascular ultrasound and optical coherence tomography. J Am Coll Cardiol Img 2009;2:473–82.
57. Kubo T, Imanishi T, Takarada S, et al. Assessment of culprit lesion morphology in acute myocardial infarction. J Am Coll Cardiol 2007;50:933–9.
58. Sum ST, Madden SP, Hendricks MJ, Chartier SJ, Muller JE. Near-infrared spectroscopy for the detection of lipid-core coronary plaques. Curr Cardiovasc Imaging Rep 2009;2:307–15.
59. Gardner CM, Tan H, Hull EL, et al. Detection of lipid-core coronary plaques in autopsy specimens with a novel catheter-based near-infrared spectroscopy system. J Am Coll Cardiol Img 2008;1:638–48.
60. Waxman S, Dixon SR, L'Allier P, et al. In vivo validation of a catheter-based near-infrared spectroscopy system for detection of lipid-core coronary plaques J Am Coll Img 2009;2:858–68.
61. Chau AH, Motz JT, Gardecki JA, Waxman S, Bouma BE, Tearney GJ. Fingerprint and high-wavenumber Raman spectroscopy in a human-swine coronary xenograft in vivo. J Biomed Opt 2008;13:040501.
62. Wilensky RL, Song HK, Ferrari VA. Role of magnetic resonance and intravascular magnetic resonance in the detection of vulnerable plaques. J Am Coll Cardiol 2006;47 Suppl:C48–56.
63. Larsen PJ, Waxman S. Intracoronary thermography. Curr Cardiovasc Imaging Reps 2009;2:300–6.
64. Takano M, Jang IK, Inami S, et al. In vivo comparison of optical coherence tomography and angioscopy for the evaluation of coronary plaque characteristics. Am J Cardiol 2008;101:471–6.
65. Kramer MC, Rittersma SZ, de Winter RJ, et al. Relationship of thrombus healing to underlying plaque morphology in sudden coronary death. J Am Coll Cardiol 2010;55:122–32.
66. Takarada S, Imanishi T, Kubo T, et al. Effect of statin therapy on coronary fibrous-cap thickness in patients with acute coronary syndrome: assessment by optical coherence tomography study. Atherosclerosis 2009;202:491–7.
67. Libby P. Molecular and cellular mechanisms of the thrombotic complications of atherosclerosis. J. Lipid Res 2009;50 Suppl:S352–7.
68. Hansson GK. Atherosclerosis—an immune disease: the Anitschkov Lecture 2007. Atherosclerosis 2009;202:2–10.
69. Jaffer FA, Libby P, Weissleder R. Optical and multimodality molecular imaging: insights into atherosclerosis. Arterioscler Thromb Vasc Biol 2009;29:1017–24.
70. Saraste A, Nekolla SG, Schwaiger M. Cardiovascular molecular imaging: an overview. Cardiovasc Res 2009;83:643–52.
71. Chang K, Jaffer F. Advances in fluorescence imaging of the cardiovascular system. J Nucl Cardiol 2008;15:417–28.

Key Words: imaging ■ intracoronary ■ plaque ■ vulnerable plaque.

▶APPENDIX

For a supplementary slide set, please see the online version of this article.